

Supplement of Geosci. Model Dev., 7, 2747–2767, 2014
<http://www.geosci-model-dev.net/7/2747/2014/>
doi:10.5194/gmd-7-2747-2014-supplement
© Author(s) 2014. CC Attribution 3.0 License.



Supplement of

Modelling the role of fires in the terrestrial carbon balance by incorporating SPITFIRE into the global vegetation model ORCHIDEE – Part 1: simulating historical global burned area and fire regimes

C. Yue et al.

Correspondence to: C. Yue (chao.yue@lsce.ipsl.fr)

Supplement material

Section S1 Supplement figures

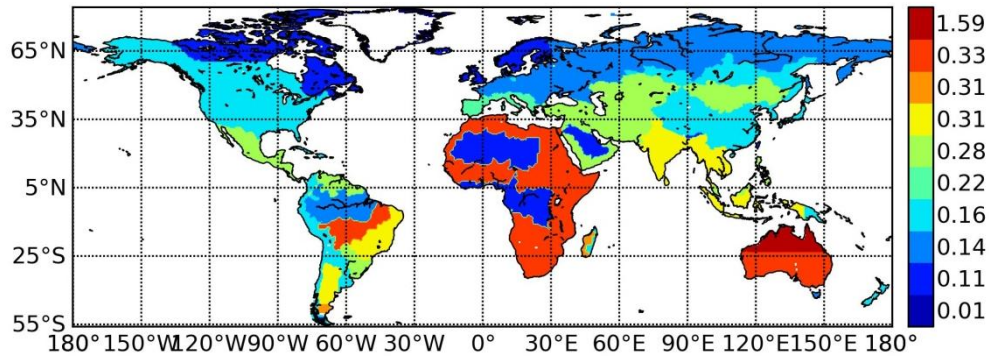


Fig. S1 The spatial distribution of a(ND) (in unit of ignitions ind⁻¹ day⁻¹) as used in the human potential ignition equation (Eq. 1 in the main text) by Thonicke et al. (2010).

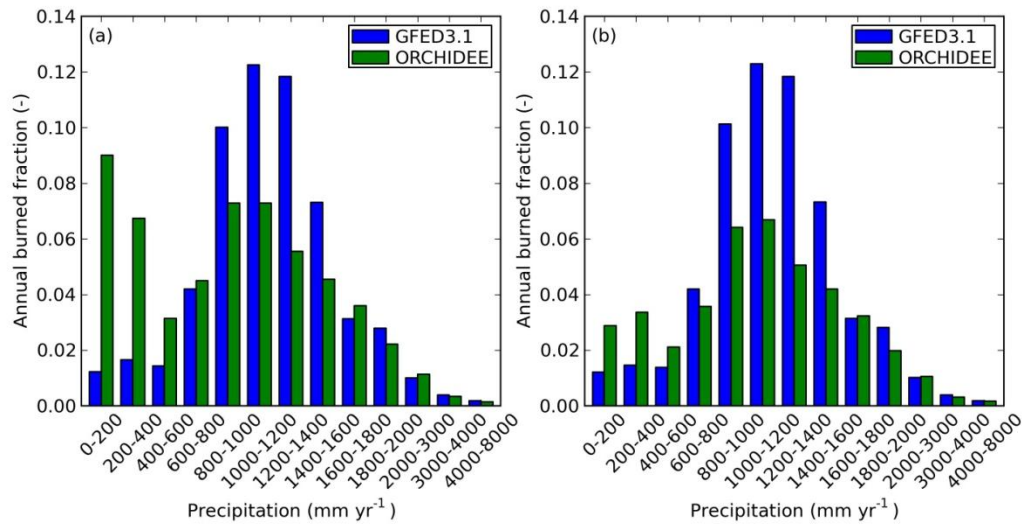


Fig. S2 Mean burned fraction over the precipitation gradient by model simulation and GFED3.1 data for (a) before and (b) after the adoption of fuel load limitation on the ignition efficiency. Burned fraction is averaged over 200-mm precipitation bins and data presented include all the pixels over the globe with burned fraction bigger than zero.

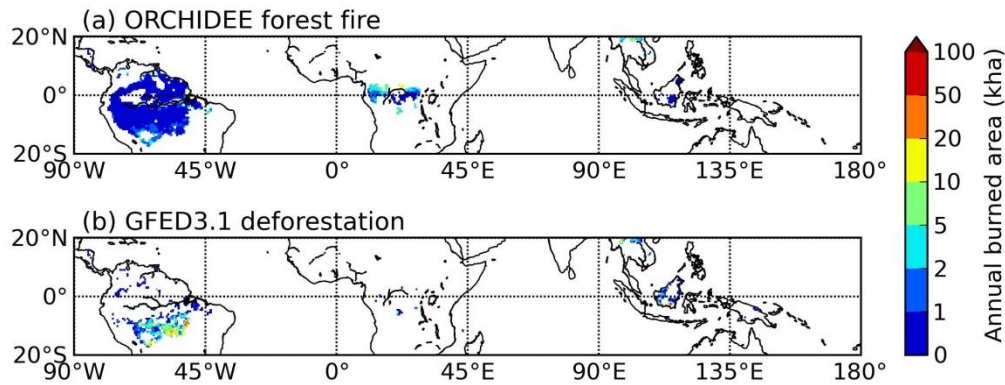


Fig. S3 Burned area in the tropical forest (20°S-20°N) given by (a) forest burned area as simulated by ORCHIDEE, and (b) estimated deforestation area by the product of GFED3.1 forest burned area and the fire persistence time as indicated by (van der Werf et al., 2010). Burned area is shown for 2000-2005 for the areas with forest coverage larger than 70% by the land cover map used in the simulation.

van der Werf et al. (2010) showed that by using the product of forest burned area and the fire persistence time as a proxy for the tropical deforestation rates, 82% of the deforested area by other independent approaches (e.g., Hansen et al., 2008) has been captured for 2000-2005. We replicated this process by using the GFED3.1 forest monthly burned area and the corresponding fire persistence time for the region of 20°S-20°N for 2000-2005. The ORCHIDEE simulated forest burned area for the same region was compared with the GFED3.1 derived deforested area. When making the comparison, only the grid cells with a forest cover >70% by the land cover map used in the simulation were included to make sure that the burned area occurred in relatively closed forest. The mean annual deforestation area for 2000-2005 for the study region by GFED3.1 was 4.0 Mha yr⁻¹, and the forest fire area by ORCHIDEE simulation is 2.7 Mha yr⁻¹ (67% of GFED3.1 deforested area).

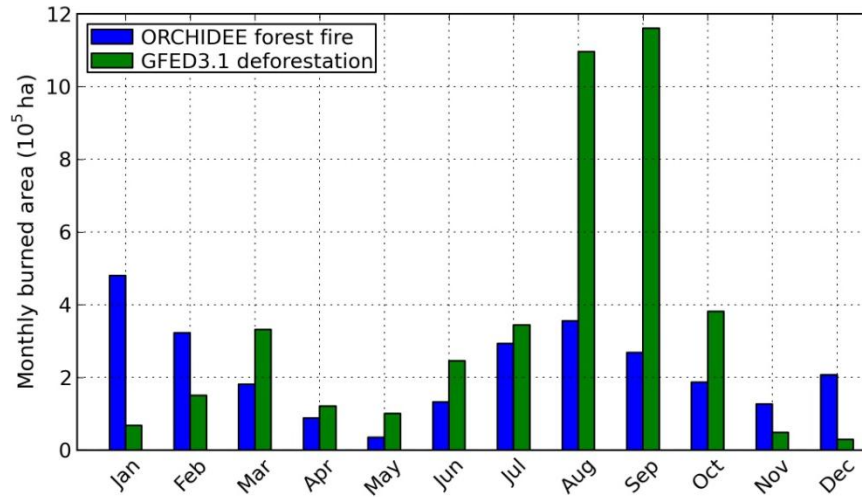


Fig. S4 Monthly burned area for the simulated forest fire (blue) and GFED3.1 deforestation area (green) for the spatial extent as in Fig. S3 averaged over 2000-2005.

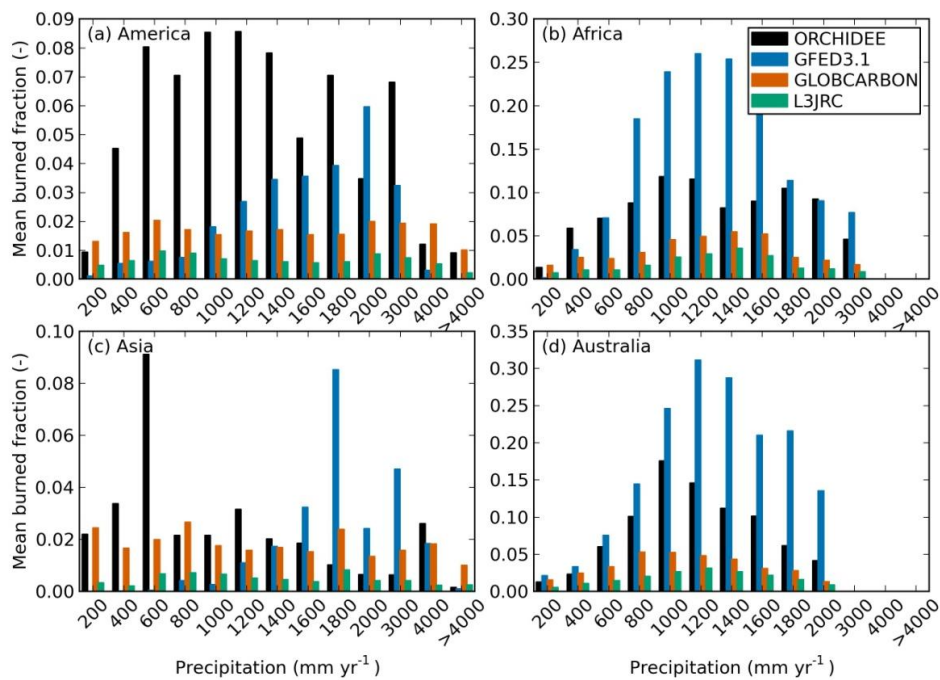


Fig. S5 Burned fraction distribution as a function of annual precipitation according to the model simulation (black), GFED3.1 (blue), GLOBCARBON (orange) and L3JRC (green) datasets for four sub-regions in the tropics and subtropics (S35-N35): (a) America; (b) Africa; (c) Asia; (d) Australia. The annual precipitation data are from CRU data and binned in 200-mm intervals.

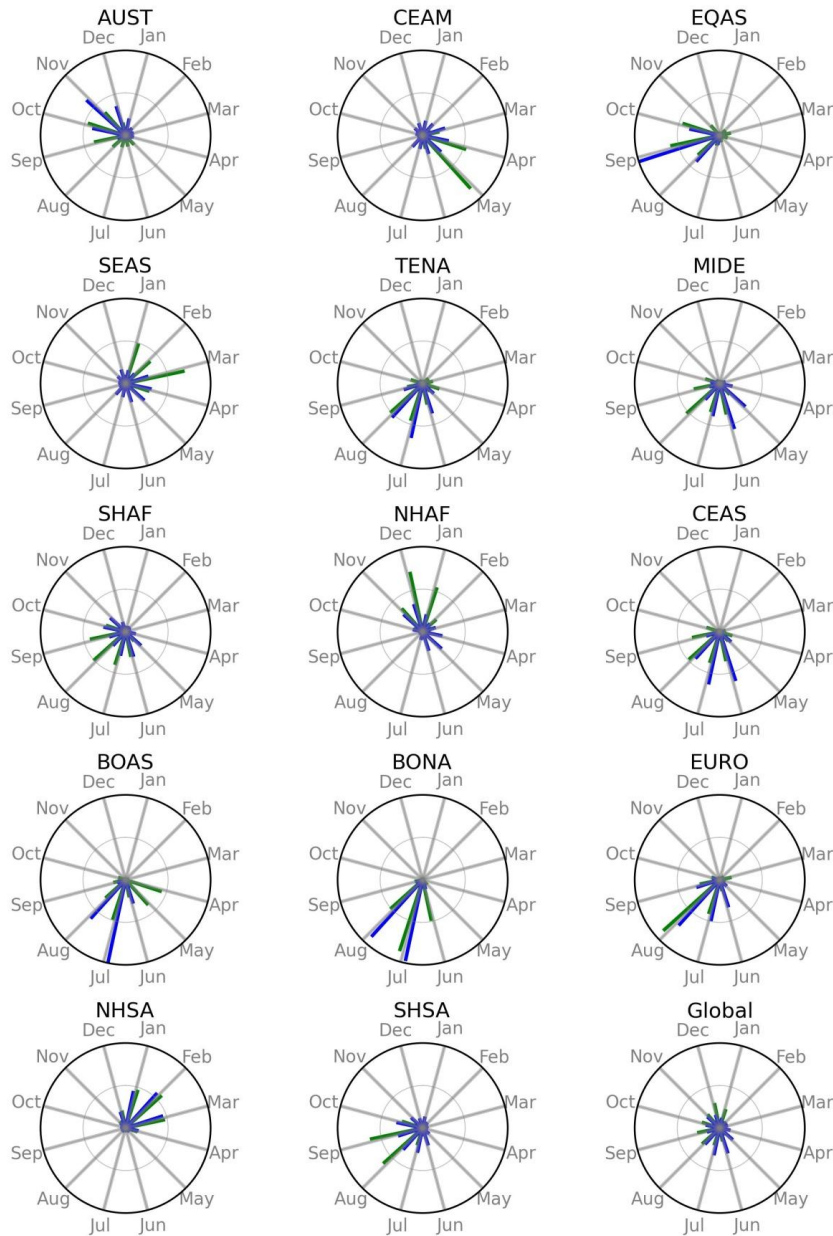


Fig. S6 Normalized monthly burned area for GFED3.1 data (green) and ORCHIDEE simulation (blue) for the globe and the different GFED3.1 regions (see Fig. 2a). The mean monthly burned areas over 1997–2009 are normalized by the annual total of each dataset and the outset black ring represents 0.5 of the annual burned area.

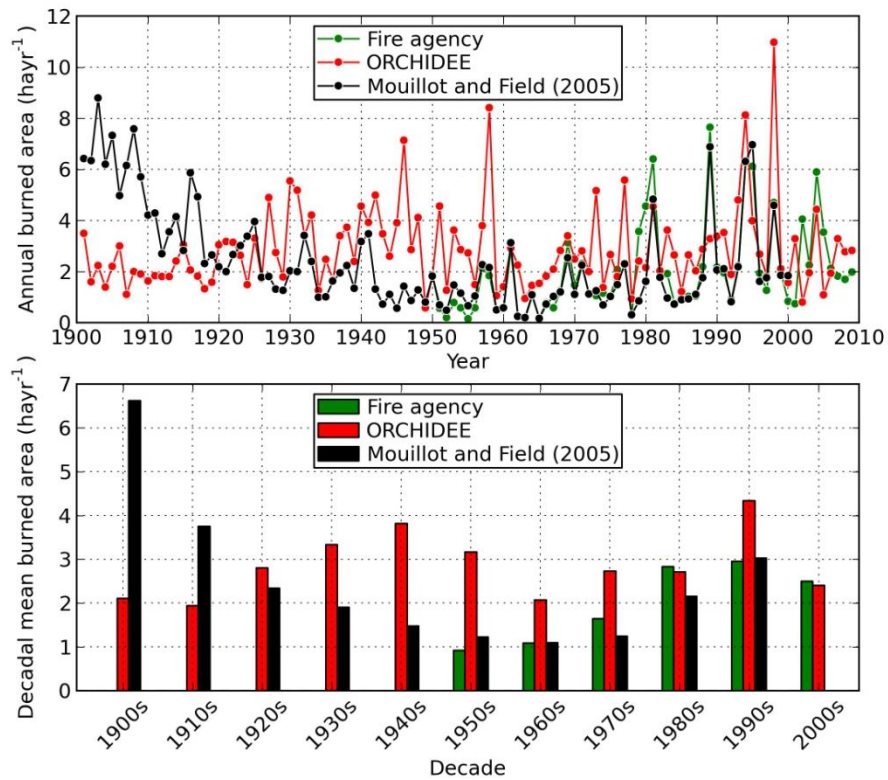


Fig. S7 Historical burned area in US Alaska and Canada as simulated by ORCHIDEE (red), as reported by Mouillot and Field, (2005) (black), and by government fire agency survey (green). The upper panel shows the annual burned area and the lower panel shows the decadal ones. After 1950, the Pearson correlation coefficient for annual burned area is 0.44 between ORCHIDEE and fire agency data, 0.57 between ORCHIDEE and the Mouillot data, and 0.92 between the fire agency and Mouillot data, all significant at 0.01 level. The correlation coefficient for the decadal burned area data after 1950s decade is 0.42 between ORCHIDEE and the fire agency data, 0.80 between ORCHIDEE and the Mouillot data, and 0.91 between the fire agency and Mouillot data. When going back prior to 1950, the model simulation and the Mouillot data show stronger divergence, probably because of the decreased reliability in the Mouillot data.

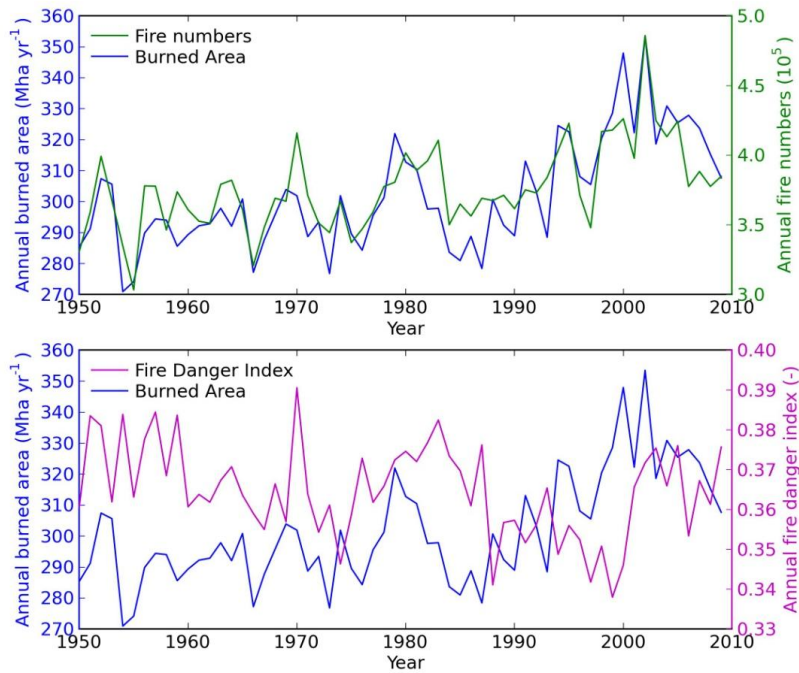


Fig. S8 The major driving factors for the global total burned area for 1950–2009. Upper panel shows the time series of global burned area (blue, left vertical axis) and the global total fire numbers (green, right vertical axis). Lower panel shows the time series of global total burned area (blue, left vertical axis) and the fire danger index (magenta, right vertical axis) as weighted by the burned area.

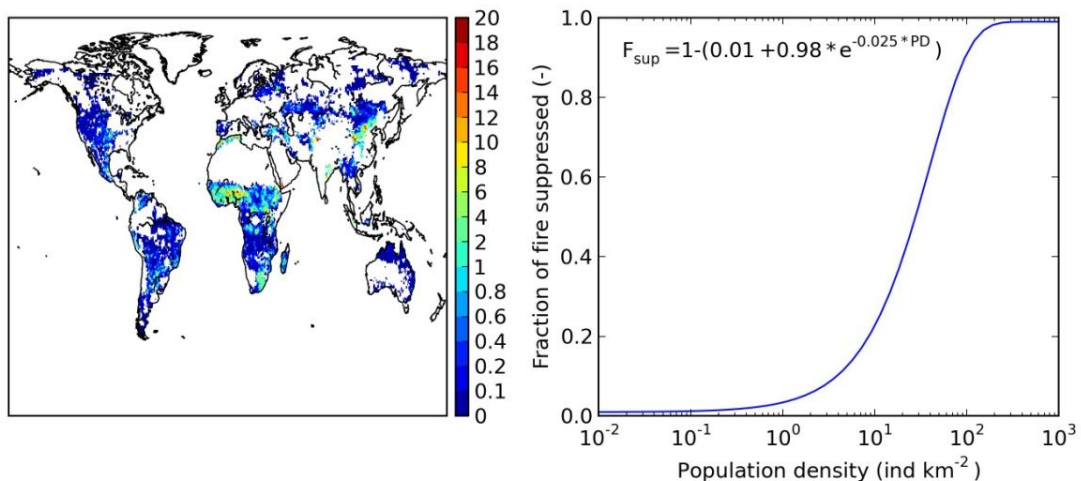


Fig. S9 The influence of applying the effect of human suppression on lightning-caused fires in the model. The left panel shows the mean annual burned fraction reduction due to the human suppression of lightning fires for 1997–2009. The right panel shows the fraction of suppressed lightning ignitions as a function of population density, following Li et al. (2012).

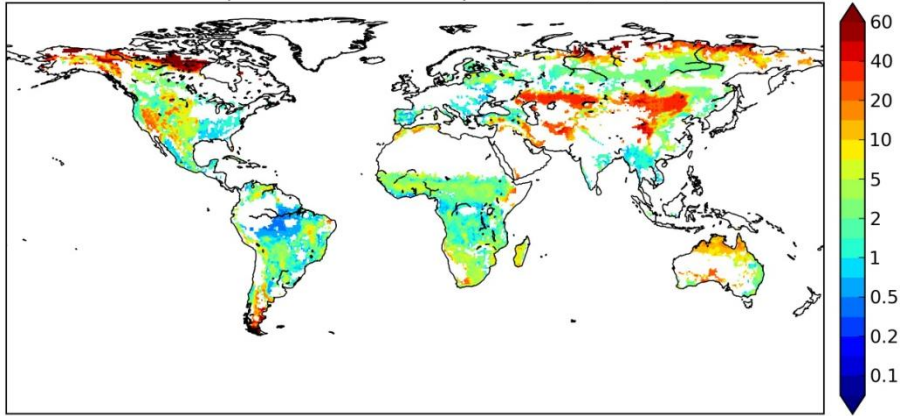


Fig. S10 Map of the 95th quantile fire forward-spread rate (m min^{-1}) as simulated by ORCHIDEE.

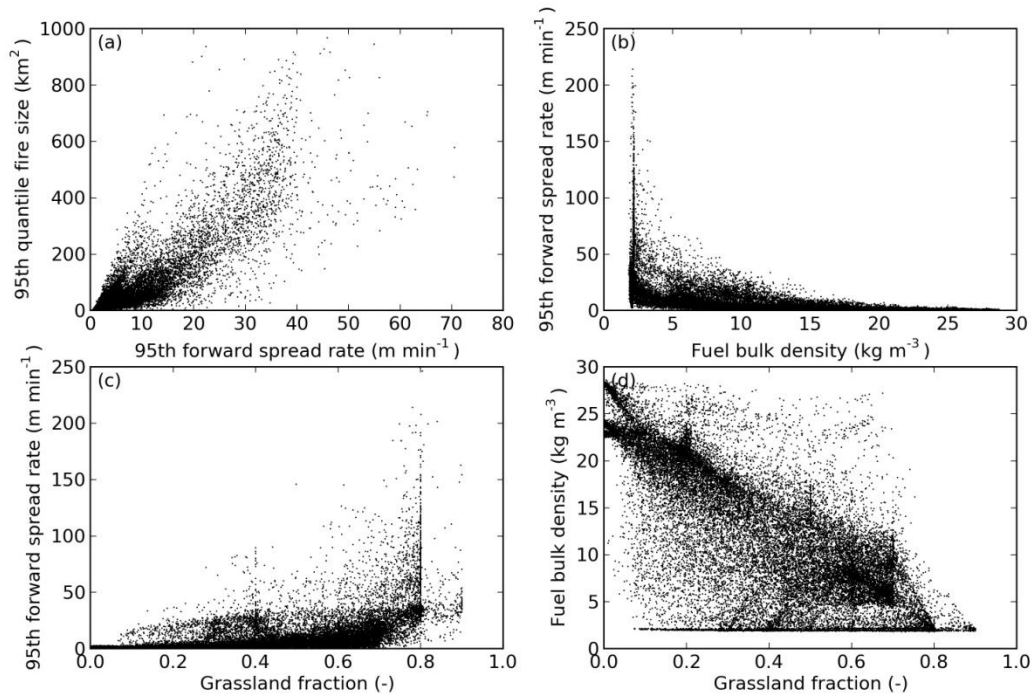


Fig. S11 Factors that influence the simulated fire size: (a) the large fire size (the 95th quantile fire size) is exponentially dependent on the 95th quantile fire forward-spread rate; (b) the 95th quantile fire forward-spread rate is inversely related to the fuel bulk density; (c) the 95th fire forward-spread rate is positively dependent on the grassland fraction (notice the threshold effect around grass fraction of ~ 0.7); (d) fuel bulk density is inversely related to the grass fraction. All data shown here are for 1997–2009 over the globe and each dot in the figure represents a 0.5° grid cell.

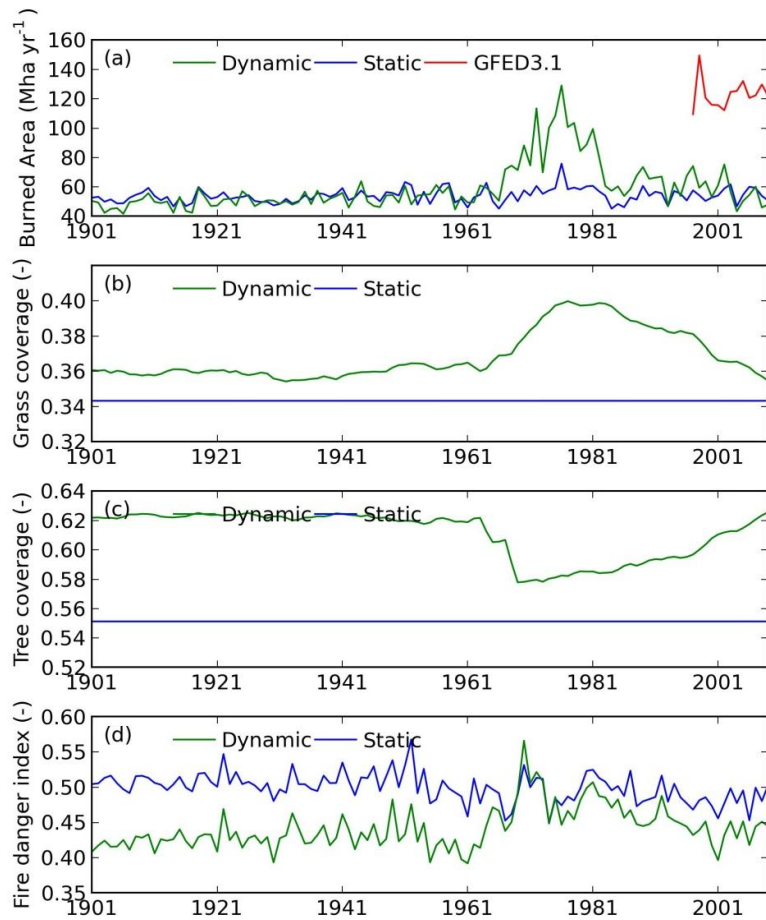


Fig. S12 Comparison of the results for simulations with the dynamic vegetation module of ORCHIDEE being switched on (green, Dynamic vegetation) and off (blue, Static vegetation) for 1901–2009: (a) simulated fire-burned area for dynamic (green) and static (blue) vegetation being compared with GFED3.1 (red) data; (b) simulated mean grass coverage change; (c) simulated tree coverage change; (d) simulated fire danger index as weighted by the burned area. The test simulation was done for southern hemisphere Africa following the same simulation protocol as described in the main text Sect. 2.3 using a slightly different PFT map by Poulter et al. (2011).

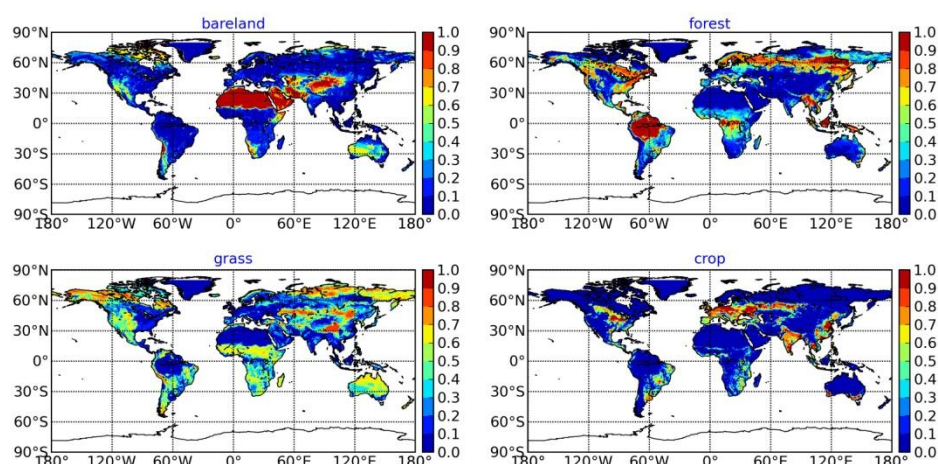


Fig. S13 The distribution of land cover types as used in ORCHIDEE model.

References:

- Hansen, M. C., Stehman, S. V., Potapov, P. V., Loveland, T. R., Townshend, J. R. G., DeFries, R. S., Pittman, K. W., Arunarwati, B., Stolle, F., Steininger, M. K., Carroll, M. and DiMiceli, C.: Humid tropical forest clearing from 2000 to 2005 quantified by using multitemporal and multiresolution remotely sensed data, *PNAS*, doi:10.1073/pnas.0804042105, 2008.
- Li, F., Zeng, X. D. and Levis, S.: A process-based fire parameterization of intermediate complexity in a Dynamic Global Vegetation Model, *Biogeosciences*, 9(7), 2761–2780, doi:10.5194/bg-9-2761-2012, 2012.
- Mouillot, F. and Field, C. B.: Fire history and the global carbon budget: a 1 degrees x 1 degrees fire history reconstruction for the 20th century, *Global Change Biology*, 11, 398–420, doi:10.1111/j.1365-2486.2005.00920.x, 2005.
- Poulter, B., Ciais, P., Hodson, E., Lischke, H., Maignan, F., Plummer, S. and Zimmermann, N. E.: Plant functional type mapping for earth system models, *Geoscientific Model Development*, 4(4), 993–1010, doi:10.5194/gmd-4-993-2011, 2011.
- Thonicke, K., Spessa, A., Prentice, I. C., Harrison, S. P., Dong, L. and Carmona-Moreno, C.: The influence of vegetation, fire spread and fire behaviour on biomass burning and trace gas emissions: results from a process-based model, *Biogeosciences*, 7(6), 1991–2011, 2010.
- Van der Werf, G. R., Randerson, J. T., Giglio, L., Collatz, G. J., Mu, M., Kasibhatla, P. S., Morton, D. C., DeFries, R. S., Jin, Y. and van Leeuwen, T. T.: Global fire emissions and the contribution of deforestation, savanna, forest, agricultural, and peat fires (1997–2009), *Atmos. Chem. Phys.*, 10(23), 11707–11735, doi:10.5194/acp-10-11707-2010, 2010.

Section S2 Investigating the role of interannual lightning variability in the model

2.1 Reconstructed lightning flashes with interannual variability

The interannual variability of lightning flashes is interpolated from the average monthly

satellite observed lightning flashes of LIS/OTD data (http://gcmd.nasa.gov/records/GCMD_lohrmc.html), by using the interannual variability of the Convective Potential Available Energy (CAPE) during the 20th century as simulated from by the 20th Century Reanalysis Project. The interpolation is done by following the method of Pfeiffer et al. (2013, Equation 1 on Page 649).

$$l_m = \begin{cases} \text{LISOTD}_m (1 + 9\text{CAPE}_{\text{anom}}), & \text{CAPE}_{\text{anom}} \geq 0 \\ \text{LISOTD}_m (1 + 0.99\text{CAPE}_{\text{anom}}), & \text{CAPE}_{\text{anom}} < 0 \end{cases}$$

where l_m the monthly lightning flash numbers for a given month, $\text{CAPE}_{\text{anom}}$ is CAPE anomaly for the concerned month being normalized to (-1,1) for 1901-2011.

We first compared the reconstructed lightning flashes with the observation by the Alaskan Lightning Detection System for 1986-2011 (Fig. S14). Their correlation coefficient is 0.48 (data not detrended).

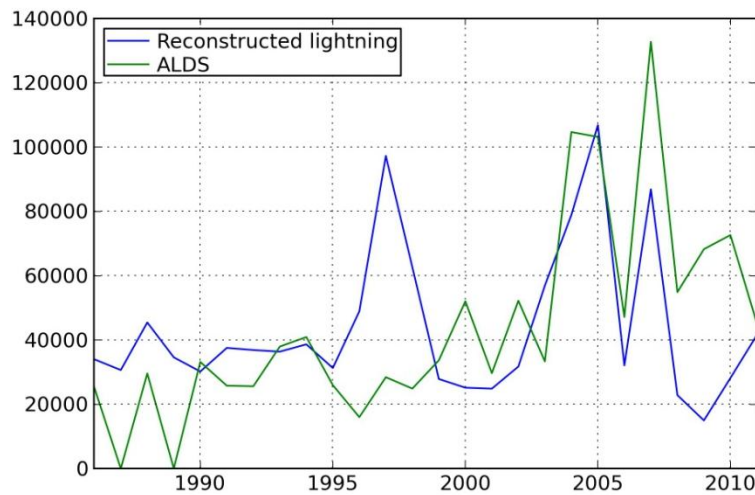


Fig. S14 The reconstructed lightning flashes compared with the lightning flashes observed by the Alaskan Lightning Detection System (ALDS) for 1986-2011. To facilitate the comparison of interannual variability, the mean annual lightning numbers of reconstructed CAPE-derived data are adjusted to have the same mean annual lightning flashes as observed by ALDS.

2.2 Compare the simulated burned area with observation data by using different lightning input data

After the reconstruction of the interannual lightning flashes, we launched a global simulation for 1901-2011 by using the new lightning data with the human ignition parameters of a(ND) (Equation 1 in the discussion paper, Page 2382) as the spatial dataset used in Thonicke et al. (2010). This simulation is denoted as "ORCHIDEE - IAVLightn", and another simulation with mean annual lighting data and the spatial a(ND) dataset is denoted as "ORCHIDEE - CONLightn". Note that the reconstruction of interannual lightning data changed the total amount of flashes, so a constant scaling factor (0.53) has been applied in the "ORCHIDEE - CONLightn" simulation, to ensure on the global scale, the same lightning ignition efficiency factor (0.03) in the original simulation to be maintained (i.e., on the global scale, the mean annual potential lightning flashes

available for ignition do not change) over 1901-2011.

Furthermore, we launched a third simulation for Alaska for 1986-2011, using the observed ALDS lightning flashes as input data, and this simulated is denoted as "ORCHIDEE - ALDS". The third simulation allows investigating the simulation improvement by using the ground-based observation of lightning flashes.

2.2.1 Compare burned area over Alaska

The simulated burned area over 1986-2011 is compared with GFED3.1 burned area data and the burned area by Alaskan fire agency, by using the Pearson correlation coefficient (r-value). The results are shown in Table S1. The increase in r-value (with the Alaskan fire agency data) by shifting from "CONLightn" to "IAVLightn" is very small (0.19 to 0.22). The r-value between simulated BA with the fire agency BA is the highest for the simulation using the ALDS input (0.5), though still lower than that of 0.66 by Pfeiffer et al. (2013) for the "Intermontane Boreal" ecoregion of Alaska who used the same lightning input (the r-value is derived by picking up the data from the Fig. 7 on Page 663 of Pfeiffer et al., 2013). Over 1950-2011, the r-value decreased from 0.41 for "ORCHIDEE - CONLightn" simulation to 0.37 for "ORCHIDEE - IAVLightn" simulation.

We found that using the CAPE-derived interannual lightning data only marginally improved the BA simulation for Alaska for 1986-2011, but using the ground-based observation of lightning data did greatly improved the simulation.

Table S1 Pearson correlation coefficient (r-value) for different annual simulated burned area data with the observation data by the Alaskan fire agency; and the r-value for different data with the ALDS observed flashes.

	1950-2011	1986-2011	Correlation with Alaskan ALDS lightning flashes (1986-2011)
Alaskan Fire Agency	1.00	1.00	0.55
GFED3.1		0.98	0.58
ORCHIDEE - CONLightn	0.41	0.19	0.20
ORCHIDEE - ALDS		0.50	0.62
ORCHIDEE - IAVLightn	0.37	0.22	0.50

2.2.2 Compare the simulated burned area with the observation for boreal North America (Alaska, US + Canada)

We examined the agreement between the simulated and observed BA for the two global ORCHIDEE simulations (with CONLightn and IAVLightn) for the boreal North America (Alaska, US + Canada). Burned area in this region is known to be dominated by lightning sources, and thus we expect the improvement in the simulation is expected to occur for this region. We used both the annual fire agency burned area data and the decadal Mouillot and Field (2005) as the observation data. The r-value between different data are shown in Table S2. Surprisingly, for all r-values, the ones by "ORCHIDEE- IAVLightn" is lower than that by "ORCHIDEE - CONLightn", suggesting that shifting from mean annual lighting data to CAPE-derived lightning data has

generally decreased the model-observation agreement in this region.

Table S2 The Pearson correlation coefficient (r-value) for the period after 1950 in terms of BA by different data (because after 1950 the fire agency data began to exist). The ***bold italic numbers*** indicate that the agreement with fire agency data deteriorated after shifting from "CONLightn" to "IAVLightn".

	ORCHIDEE - CONLightn	ORCHIDEE - IAVLightn
Annual correlation (n=61)		
ORCHIDEE ~ Fire Agency	<i>0.44</i>	<i>0.41</i>
ORCHIDEE ~ Mouillot & Field (2005)	<i>0.57</i>	<i>0.44</i>
Mouillot & Field (2005) ~ Fire Agency	0.92	0.92
Decade correlation (n=6)		
ORCHIDEE ~ Fire Agency	<i>0.42</i>	<i>0.27</i>
ORCHIDEE ~ Mouillot & Field (2005)	<i>0.81</i>	<i>0.62</i>
Mouillot & Field (2005) ~ Fire Agency	0.91	0.91

2.2.3 Compare the simulated burned area with the observation over the 20th century for different Mouillot & Field (2005) regions

We compared the decadal r-value over the 20th century with the Mouillot and Field (2005) reconstructed BA data as shown in Table S3. When examining the r-value for different regions, for some regions the BA are rather poorly simulated by the model with negative r-values (indicating anti-phase between model and observation). Over the whole globe, the r-value after shifting to IAVLightn slightly decreased (by 0.1). Of the 14 region, the r-values decreased after shifting to IAVLightn for 6 regions, with 2 regions showing no change in r-value, and 6 regions with increase in r-value. On the global scale, the model-observation agreement decreased after shifting to the CAPE-derived lightning data, and for half the regions the agreement increased and the other half decreased.

Table S3 The Pearson correlation coefficient between simulated decadal BA and Mouillot and Field (2005) reconstructed BA over the 20th century (n=11). The negative r-values (poor simulation and anti-phase between model and data) and the decrease in r-value after shifting to IAVLightn are shown in red.

	CONLightn (r1)	IAVLightn (r2)	Improvement (r2-r1)
Global	0.6	0.5	-0.1
Australia	-0.4	-0.5	-0.1
BONA	-0.4	-0.5	-0.1
BOAS	-0.1	0.3	0.4
India	0.8	0.6	-0.2
SouthEastAsia	0.0	0.4	0.4
CentralAsia	0.4	0.3	-0.1
WestUS	-0.6	-0.9	-0.3
EastUS	0.1	0.4	0.3
EastAsia	-0.6	-0.7	-0.1

MiddleEastNorthAfrica	-0.6	-0.5	0.1
Africa	-0.5	0.0	0.5
CentralSouthAmerica	0.8	0.8	0.0
SouthAmerica	-0.6	-0.2	0.4
Europe	0.1	0.1	0.0

2.2.4 Compare the annual simulated burned area with GFED3.1 data for 1997-2009 for the 14 GFED regions

The Pearson correlation coefficients between annual simulated BA with GFED3.1 BA have been calculated for different GFED regions and the globe for simulations with CONLightn and IAVLightn (Table S4). The annual time series of burned area are shown in Fig. S15. Over the globe, the model-observation agreement decreased, and for only two out of the 14 regions, the r-value increased after shifting to IAVLightn.

Table S4 The Pearson correlation coefficient (r-value) between annual simulated BA with the GFED3.1 data for different GFED regions. The negative r-values (i.e., poor simulation of model) and the decrease in r-value after shifting to IAVLightn are shown in red.

	CONLightn (r1)	IAVLightn (r2)	Improvement (r2-r1)
Global	0.5	0.3	-0.2
BONA*	0.5	0.7	0.2
TENA	0.3	0.1	-0.2
CEAM	0.2	-0.1	-0.3
NHSA	-0.1	0.0	0.2
SHSA	0.3	-0.5	-0.9
EURO	-0.1	-0.1	0.0
MIDE	0.3	0.1	-0.2
NHAF	0.2	-0.2	-0.3
SHAF	0.0	0.0	0.0
BOAS	0.4	0.0	-0.4
SEAS	-0.1	-0.4	-0.3
CEAS	0.2	0.0	-0.2
EQAS	1.0	1.0	0.0
AUST	0.2	-0.1	-0.3

* This is not in contradiction with results presented in Section 2.2 as the spatial extent of boreal North America and the BONA here are slightly different. The BONA includes part of the western US where the model overestimated BA.

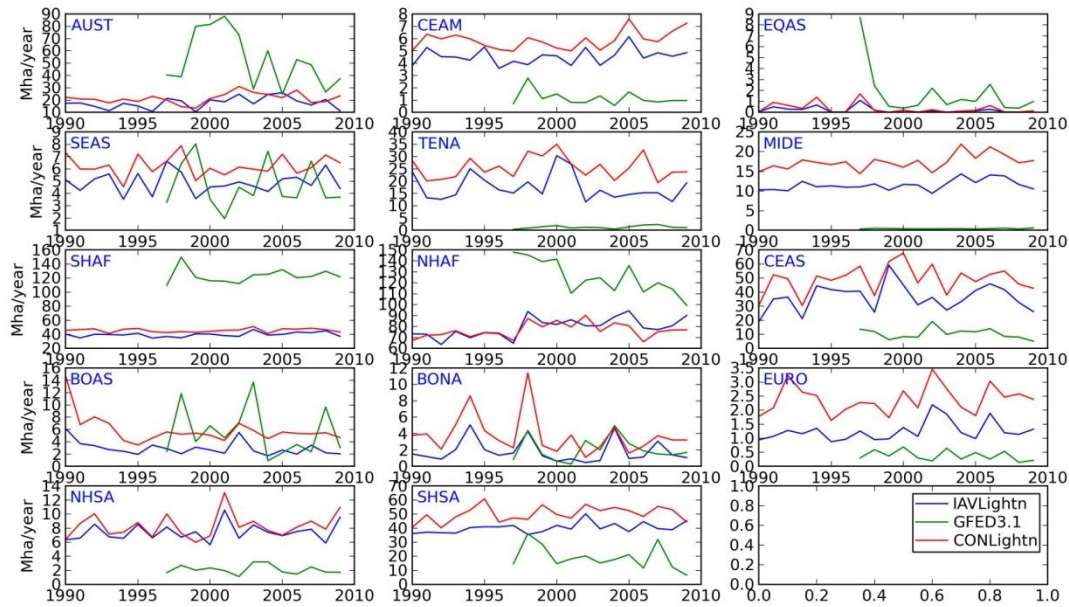


Fig. S15 The annual BA time series for different GFED regions for 1997-2009 by GFED3.1 data, and the two model simulations ("ORCHIDEE - CONLightn" and "ORCHIDEE - IAVLightn").

2.2.5 Compare simulated global BA with GFED3.1 data

The total global BA is 273 Mha yr^{-1} according to "ORCHIDEE - IAVLightn" simulation for 1997-2009 (compared with 342 Mha yr^{-1} for "ORCHIDEE - CONLightn" and 349 Mha yr^{-1} for GFED3.1). Fig. S16 shows the annual BA time series of ORCHIDEE and GFED3.1, with the r -value of linearly detrended annual time series between "ORCHIDEE - IAVLightn" and GFED3.1 is 0.46 (compared with 0.57 between "ORCHIDEE - CONLightn" and GFED3.1). There is no significant change in the spatial distribution of fires (pixel-to-pixel correlation between "ORCHIDEE - IAVLightn" and GFED3.1 is 0.481, and 0.475 between "ORCHIDEE - CONLightn" and GFED3.1). Thus if the global total potential available lightning ignitions over 1901-2011 were conserved in the simulation, the simulated global burned area decreased from 342 to 273 Mha yr^{-1} for 1997-2009 when shifting to the CAPE-derived lighting data, and the model-GFED3.1 agreement in the global burned area interannual variability decreased.

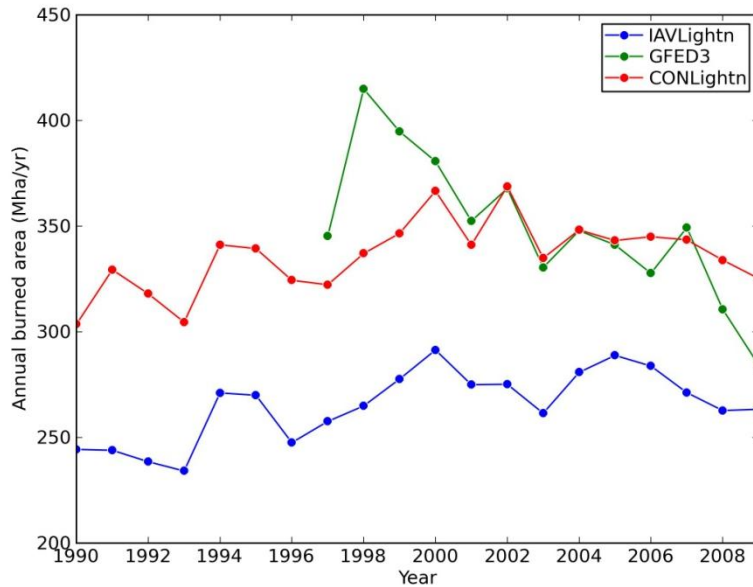


Fig. S16 Annual global burned area by model simulation and as given by GFED3.1 data for 1990-2009.

2.3 Summary

We have followed the method proposed by Pfeiffer et al. (2013) and reconstructed the total lightning flashes with interannual variability for 1901-2011 by using the CAPE data. The new CAPE-derived lightning data moderately agreed with the ground observations of lightning flashes for Alaska for 1986-2011. However, the model-observation agreement for the burned area in Alaska for 1986-2011 has only been marginally improved by using the new CAPE-derived lightning data, compared with repeating the mean annual lightning data without interannual variability being included. For 1950-2011, the model-observation agreement slightly decreased after shifting to the new CAPE-derived lightning data. Large improvement in the simulation was found when the model was directly driven by the locally observed lightning data.

The agreement of simulated burned area with the observation data for 1950-2011 for the boreal North America (i.e., US Alaska + Canada) generally decreased after shifting to the CAPE-derived lightning data, either on annual or decadal basis. Over the 20th century, the shifting of lightning data decreased the agreement of simulated decadal burned area with the Mouillot and Field (2005) reconstruction for half of the 14 regions and increased for the other half. Especially, over 1997-2009 when the observation data by the GFED3.1 is more credible than the 20th century reconstruction, shifting of the lightning data decreased the agreement of annual simulated and observed burned area for the globe and for most of the regions.

The fact that the CAPE-derived lightning data does not systematically improve the model performance could be linked with several explanations. First, despite the physical linkage between the CAPE (atmospheric instability) and the lightning activity, the approach (equation) used here might not apply for all the regions of the globe, as it's mainly derived by the lightning observation in Alaska. Second, the errors in the CAPE data provided by the 20th Century Reanalysis Project might also contribute. Third, the uncertainties of internal model processes might have counteracted some of the expected improvement gains. For example, in Alaska, the complete

replacement by local lightning observations only increased the model-observation correlation from 0.19 to 0.5, while less improvement in the lighting input data (the correlation of 0.48 between ALDS and CAPE lightning data could be considered as an improvement in the input data compared with the otherwise mean annual lightning data) leads to nearly negligible improvement in the simulation result (r-value 0.19 to 0.22).